



Universiteit
Leiden
The Netherlands

Correlative light and electron microscopy : strategies and applications

Driel, L.F. van

Citation

Driel, L. F. van. (2011, October 11). *Correlative light and electron microscopy : strategies and applications*. Retrieved from <https://hdl.handle.net/1887/17922>

Version: Corrected Publisher's Version

License: [Licence agreement concerning inclusion of doctoral thesis in the Institutional Repository of the University of Leiden](#)

Downloaded from: <https://hdl.handle.net/1887/17922>

Note: To cite this publication please use the final published version (if applicable).

Chapter 5

Actin coated secretory granules studied by cryo- correlative microscopy

This chapter describes work in progress.

Abstract

Following stimulation for regulated exocytosis, the filamentous actin in the apical region of pancreatic acinar cells reorganizes to coat zymogen granules. These actin coated granules (ACGs) have been observed and studied in several other models of regulated exocytosis as well. Nevertheless, their function remains a subject of debate, not in the least because of the short-lived nature of the actin coats, which are therefore difficult to image. To elaborate on a possible function, the present study used correlative cryo-fluorescence microscopy and cryo-electron microscopy (cryo-CLEM) to visualize the ultrastructure of ACGs. Specimens consisted of zymogen granules isolated from rat pancreatic tissue, and stimulated *in vitro* for exocytosis to give rise to ACGs. For cryo-fluorescence microscopy (cryo-FM), we labeled filamentous actin with fluorescent phalloidin. The cryo-CLEM procedure enabled us to locate ACGs in vitreous samples, and subsequently zoom in on the ultrastructure of the actin coats by cryo-EM. The samples illustrate the added value of the cryo-CLEM workflow, since ACGs were rarely present in the sample, and difficult to detect in EM due to their electron translucency. The results show that actin coats assemble around complete zymogen granules *in vitro*, indicating that ACGs arise before actual exocytosis. The complete zymogen granules were, however, not suitable for tomography due to their thickness. Cryo-electron tomography was instead performed on actin coats that were present on granules that were damaged during sample preparation. Surprisingly, these ACGs reproducibly showed to consist of long actin filaments bundled parallel to form an actin ring. Whether the actin rings represent a physiological phenomenon that is also associated with regulated exocytosis is yet to be elucidated.

Introduction

Regulated exocytosis is a process whereby bioactive molecules, stored in membrane-bound secretory granules, are released from the cell in response to a chemical or mechanical trigger that causes fusion of the secretory granule membrane with the plasma membrane. It is a tightly controlled process, that ensures digestive enzymes, hormones, proinflammatory cytokines, etc. are secreted only when necessary, and in specific locations. As a model system, zymogen granules containing inactive digestive enzymes are synthesized by, and secreted from pancreatic acinar cells. When digestive enzymes are demanded in the small intestines, the granules travel to and fuse exclusively with the apical side of the plasma membrane. Here, the enzymes are collected in ducts that lead to the small intestines.

The exocytotic event is mediated by multiple docking and fusion proteins. These include the SNAP (soluble N-ethylmaleimide-sensitive fusion protein attachment protein) and SNARE (SNAP receptor) proteins. According to the widely accepted SNARE hypothesis (Ferro-Novick and Jahn, 1994; Rothman and Sollner, 1997), transmembrane SNARE proteins present on the vesicle and target membranes pair up to drive membrane fusion. Accessory proteins such as Sec1/Munc18 (SM) proteins, Rab GTPases, synaptotagmin and complexins are thought to regulate this process (Cai et al., 2007; Malsam et al., 2008; Martens et al., 2007; Melia, 2007).

Another actor in the exocytosis process that has received considerable attention in literature is the cytoskeletal component actin (Aunis and Bader, 1988; Burgoyne and Cheek, 1987; Valentijn et al., 1999b). In resting conditions, actin aligns the apical plasma membrane in a tight meshwork. Evidence suggests that this terminal actin web forms a barrier between the zymogen granules and the plasma membrane, to prevent exocytosis (Aunis and Bader, 1988; Muallem et al., 1995). In agreement with this, actin stabilizing agents like phalloidin and jasplakinolide greatly reduce the release of amylase (Muallem et al., 1995; Valentijn et al., 2000). On the other hand, the role of actin seems not merely to constitute a barrier, but has also been postulated a more active role during secretion. It was proposed to mediate vesicle recruitment to the plasma membrane (Bi et al., 1997; Poucell-Hatton et al., 1997) or provide contractile forces for the extrusion of secretory products (Segawa and Yamashina, 1989).

In accordance with this active role for actin in exocytosis, actin filaments not only disassemble following exocytosis stimulation; fluorescence microscopy has shown the simultaneous assembly of actin filaments into circular actin coats aligning the apical plasma membrane (Nemoto et al., 2004; Valentijn et al., 2000). Since these actin coats were thought to surround the zymogen granules, they were called actin coated granules (ACGs). ACGs seem to have a fundamental function in regulated secretion, as they have also been observed in other models of regulated exocytosis, such as oocytes (Becker and Hart, 1999; Yu and Bement, 2007), alveolar cells (van Weeren et al., 2004) and lacrimal cells (Jerdeva et al., 2005). However, the function of ACGs has

been subject of debate. Several studies have suggested a role in the pre-fusion phase of exocytosis. Supporting these views is that many organelles are intrinsically capable of actin nucleation activity, both *in vivo* and *in vitro* (for a review, see Taunton, 2001). In pancreatic acinar cells, actin coats would facilitate the movement of the granules across the terminal web (Valentijn et al., 2000). Actin coats were later proposed to assemble during docking of neuro-endocrine secretory granules to function in the dynamics of a following fusion pore (Gasman et al., 2004), and to enclose homotypic fusion intermediates in lacrimal cells (Jerdeva et al., 2005). In *Dictyostelium* cells, actin coating of post-lysosomal vesicles has been proposed to proceed in two steps; a first phase of weak actin coating followed by a more intense coating upon docking of the granule for exocytosis (Lee and Knecht, 2002).

The variety of postulated functions of ACGs as actors in the pre-fusion phase of exocytosis is complicated further by studies that assign the coats a role in post-fusion events. Turvey and Thorn (2004) and Nemoto et al. (2004) showed that pancreatic ACGs were always accessible to fluorescent dextran in the extracellular medium, and have thus already fused with the plasma membrane. They suggest that the actin coats stabilize the vesicle membrane during fusion (Nemoto et al., 2004), or facilitates sequential exocytosis (Pickett and Edwardson, 2006). For both alveolar cells and *Xenopus* eggs, actin coat formation was proposed to have a dual function: besides coat compression as a necessity for content release, the coat also facilitated vesicle retrieval for compensatory endocytosis (Miklavc et al., 2009; Sokac et al., 2003).

Valentijn et al. (2000) previously demonstrated that actin coats are able to assemble in a pancreatic homogenate enriched in zymogen granules. In the current study, we set out to study the ultrastructure of the actin coats in this *in vitro* system to learn more about a possible role for these structures. We used a technique that was recently developed in our laboratory for correlative cryo-fluorescence microscopy and cryo-electron tomography (chapter 4). This technique allowed us to first localize ACGs in cryo-FM using fluorescent phalloidin, and subsequently retrieve the exact ACGs in cryo-EM for ultrastructural examination. The use of cryo-EM facilitated high resolution imaging of the actin coats, circumvented sectioning of the granules, and, importantly, prevented the use of osmium tetroxide, which is known to fragment actin filaments (Maupin-Szamier and Pollard, 1978).

We show that zymogen granules intrinsically have the ability to form actin coats around their limiting membranes, suggesting that the process of coating starts before granule fusion. Unexpectedly, the contents of zymogen granules was too dense to allow direct cryo-electron tomography of the unsectioned granules. However, actin coats were also seen to surround granules that had been damaged during the homogenization process. Tomograms of these actin coats revealed that they were not spheres of actin coating the complete granule, but instead were rings of actin only several filament layers thick. The cryo-electron tomograms also revealed numerous clathrin-coated vesicles surrounding the actin rings, which indicate *in vitro* membrane retrieval of the broken granules. Although further experiments are necessary to show whether the

intact granules also display actin rings, an actin ring that spontaneously forms around the granule membranes in response to stimulation is an interesting phenomenon to consider during future exocytosis-linked actin studies.

Material and Methods

Actin coating of secretory granules in tissue extracts

Pancreata of male rats between 150-200 g (Sprague-Dawley) were treated as has been described before (Valentijn et al., 2000), with the exception that the resulting zymogen granule fraction was not chemically fixed. Briefly, pancreata were homogenized in homogenization buffer (pH 6.8) including CaCl_2 , centrifuged to generate postnuclear supernatant (PNS) fractions, supplemented with 2 mM ATP and 100 μM GTP[γS], and incubated for 20 min at 37°C. In some experiments, GTP[γS] was omitted from the fraction. The samples were now transferred in 500 μl portions to tubes containing dried, alexa488-bound phalloidin (Invitrogen, Breda, the Netherlands) to a final concentration of 1:25, and incubated for 15 min at RT. Following the incubation, the tubes were centrifuged for 10 min at 1,000 \times g to generate a crude particulate fraction enriched in zymogen granules. The supernatant was removed and the particulate was resuspended in 1 ml of homogenization buffer. This final solution was further processed for either confocal fluorescence microscopy or cryo-fluorescence microscopy.

In several experiments, we followed a slightly different protocol to eliminate more plasma membrane from the fractions before the incubation with ATP and GTP[γS]. In these experiments, we ultracentrifuged half of the PNS at 100,000 \times g for 60 minutes. This step spins down all membranes and contaminants, and leaves a supernatant of pure cytosol. The other half of the PNS was centrifuged for 10 minutes at 1,000 \times g to generate a zymogen granule fraction. The cytosol and zymogen granule fractions were afterwards combined, and incubated as described above with ATP, GTP[γS], and phalloidin, followed by centrifugation and resuspension in 1 ml homogenization buffer.

Confocal Fluorescence Microscopy

A droplet of the zymogen granule fraction was immediately brought onto a microscope slide and covered by a glass coverslip. Samples were observed with a Leica SP2 confocal system (Leica, Wetzlar, Germany) using a $\times 63$ oil-immersion objective. Images were acquired with a Photometrics CH250 CCD camera.

Sample preparation for cryo-CLEM

Golden finder grids (type H6 or HF15 of Agar Scientific Ltd., Essex, United Kingdom), which were coated with formvar and carbon and a layer of 15 nm colloidal gold particles as fiducials for

electron tomography, were glow discharged just prior to vitrification. Then, a 3 μ l droplet of the zymogen granule solution was brought onto the grids, the samples were blotted and vitrified by plunge-freezing in liquid ethane using a Vitrobot (FEI Company, Eindhoven, the Netherlands), in which the climate chamber was kept at 100% humidity. Grids with vitrified samples were stored in liquid nitrogen until further use in cryo-fluorescence microscopy.

Cryo-Fluorescence Microscopy

A cryo-FM stage was used that was described previously (chapter 4). The stage was mounted on a Leitz DMRB fluorescence microscope, and samples were viewed using a $\times 100$ dry objective lens with a working distance of 4.7 mm, and a numerical aperture of 0.75. Images were acquired using a Leica camera type DFC 350FX. For making image stitches, it was useful to have a larger field of view. We therefore used an adapter piece attached to the camera that can zoom out to 0.55 \times . The image stitches were typically build up of 3 to 10 images, and were made to include several grid bar corners and a character of the finder grid. Image stitches were afterwards aligned using the automatic photomerge tool in Photoshop. After imaging, samples were again stored in liquid nitrogen until further observation with cryo-EM.

Cryo-Electron Microscopy and -Tomography

After examination with cryo-FM, vitreous pancreatic samples on grids were transferred to a TEM cryoholder type 626 (Gatan, Pleasanton, USA) and brought into a Tecnai F20 microscope (FEI company, Eindhoven, the Netherlands), equipped with a FEG and a post-column 2k x 2k camera with energy filter (Gatan 2002), and operated at 200 kV. To retrieve the locations of interest where ACGs were identified in cryo-FM, we used a two steps approach: 1) We globally recognized the region by manually finding the character of the finder grid that was included in a cryo-FM image stitch (see above). 2) We then carried on the refined retrieval with the LCOTRAS software that was developed in our lab (chapter 4). This software uses the EM coordinates of the grid bar corners, or other features recognized in the cryo-FM image stitches, to calculate the EM coordinates of a specific location of interest. On the locations of interest, a low magnification EM image was taken in which we could recognize the ACG of interest. We then carried on with high magnification cryo-EM imaging, or, alternatively, cryo-electron tomography of these structures.

Cryo-electron tomograms were typically taken from $+55^\circ$ to -55° , with 1.5° or 2° increment using Xpolre3D (FEI Company). Total electron dose was always kept below 90-100 electrons per \AA^2 . Tilt series were aligned, reconstructed into a 3D volume, and denoised by nonlinear anisotropic diffusion filtering using the IMOD software package (Kremer et al., 1996). Several reconstructed tomograms were afterwards modeled using the AMIRA visualization package (TSG Europe). Modeling was done by first roughly masking the structures, and subsequently thresholding the densities within this mask.

Results

In this study, the aim was to investigate the organization of actin filaments in the actin coats that enclose zymogen granules in vitro in response to stimulation. The structure can further our understanding of actin coating of pancreatic zymogen granules; how does this progress and what is its function? We opted for high-resolution imaging using cryo-electron tomography. However, ACGs are rarely observed even by fluorescence microscopy in thick sections of pancreatic tissue. To increase the incidence of ACGs somewhat, it is possible to stimulate actin coating in an in vitro, cell-free system wherein zymogen granules are concentrated together (Valentijn et al., 2000). Such an in vitro system also circumvented sectioning, and was therefore suitable for direct imaging using cryo-EM.

Stimulated pancreatic fractions display actin coats

To get an idea of the composition of the homogenates before and after secretory stimulation, we examined the fractions by cryo-EM and fluorescence microscopy of fluorescent phalloidin. Because GTP is necessary for the stimulatory signal of Ca^{2+} to have an effect on the tissue (Valentijn et al., 2000), we could compare stimulated and non-stimulated tissue by the presence or absence of GTP[γ S] in the homogenate.

The two fractions seemed identical in cryo-EM. Both stimulated and unstimulated displayed zymogen granules as dense protein cores that were sometimes enclosed in tight limiting membranes (fig. 1A), and sometimes in membranes that had openings (fig. 1B). The opened granule membranes thus appeared regardless of secretory stimulation, and thereby suggest that they are damaging artefacts caused by preparation and not physiological fusion events between granules and pieces of plasma membrane present in the homogenate. However, to have more evidence that this latter option can be ruled out, we repeated the experiments with an extra step of ultracentrifugation, to clear the homogenate from any membranes left behind in the PNS. The zymogen granules in these fractions again looked identical and regularly had open membranes, which supports the idea that open membranes do not result from in vitro exocytosis. In all fractions, the granules, both intact and opened, had the tendency to cluster together with each other and different cellular material within the homogenate, like mitochondria and ER fragments (fig. 1A and B). However, we failed to identify actin associated with zymogen granules, either intact or damaged, in these samples.

Confocal imaging of fluorescent phalloidin in the stimulated and unstimulated fractions, on the other hand, did reveal a clear difference. Whereas the unstimulated fractions showed regular patches of unstructured F-actin, the stimulated material also showed perfect F-actin rings (fig. 1C and C'). The rings were mostly clustered together with the F-actin patches, but were sometimes completely isolated. The same was again true for the ultracentrifuged cytosol fractions, although actin patches and actin rings were scarcer (fig. 1D and D').

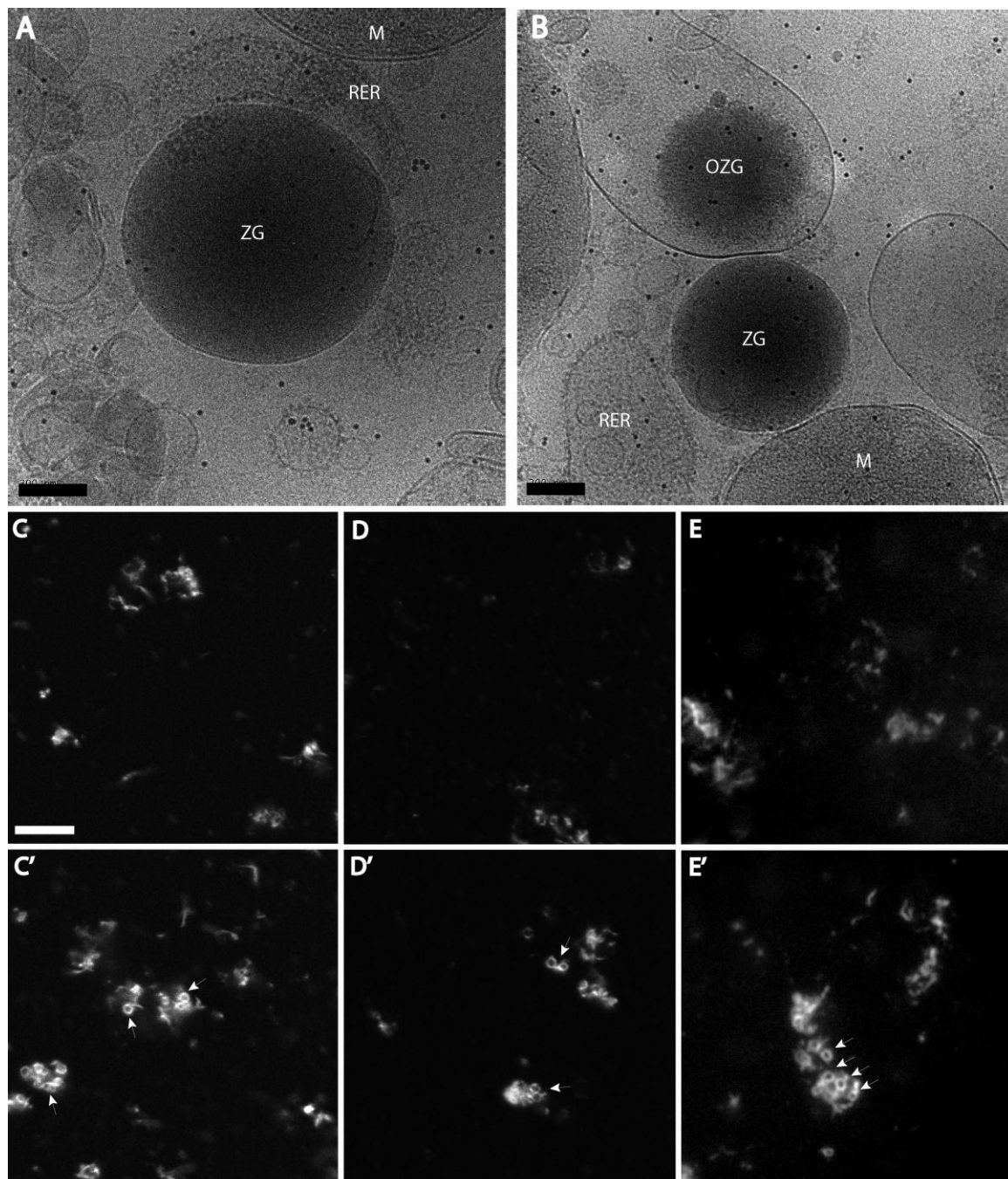


Figure 1. Cryo-EM and confocal imaging of pancreatic homogenates enriched in zymogen granules. A) and B) Cryo-EM micrographs of zymogen granules in unstimulated homogenates. Granules appeared either intact (ZG), or with an opened delineating membrane (OZG). The homogenate also contained contaminants like mitochondria (M), remnants of rough ER (RER), and many proteins. Also apparent as small circular electron densities are 15 nm gold particles, which were used as fiducial markers in electron tomography. C) and C') Confocal micrograph of unstimulated (C) and stimulated (C') pancreatic homogenate, fluorescently labeled for F-actin with phalloidin-alexa 488. Small patches of F-actin were observed regularly in unstimulated sample, whereas the stimulated fractions showed additional round actin coats (arrows). D) and D') Confocal micrographs of unstimulated (D) and stimulated (D') pancreatic homogenates, in which the PNS was ultracentrifuged to eliminate left over membranes and contaminants. The fraction also contained actin patches, and actin coats if the fraction was stimulated for exocytosis (arrows). E) and E') Cryo-FM micrographs of plunge-frozen stimulated (E) and unstimulated (E') pancreatic homogenates. The vitreous samples show the same features as the fractions imaged by confocal imaging. Scale bars represent 200 nm in (A) and (B), and 5 μ m in (C).

Thus, although the confocal images revealed actin coats in stimulated material, no such assemblies were found in cryo-EM of the same material. Since the actin rings were relatively scarce, and actin is moreover difficult to observe in cryo-EM, it was plausible that we did not come across the actin coats in cryo-EM, or that we simply did not recognize them. To examine this, we next prepared the cryo-EM samples with the addition of fluorescent phalloidin, and observed them with cryo-FM. With this technique, the stimulated fractions again contained ring-shaped actin coats (fig. 1E and E'). The ACGs had a diameter of $0.8 \pm 0.1 \mu\text{m}$ (determined on 150 ACGs during 4 different experiments), which corresponds to that of ACGs in pancreatic tissue sections (Valentijn et al., 2000).

Cryo-CLEM of Actin Coats

We next set out to combine cryo-FM and cryo-EM in a cryo-CLEM experiment, so that the former technique could locate the actin coating events, whereas the latter could provide the ultrastructural data.

By applying the cryo-CLEM workflow described in chapter 4, we were able to detect the actin coats in the cryo-EM samples. We separated four different groups based on their ultrastructural appearance. In the first, group, which composed about 50%, actin coats surrounded intact, mature zymogen granules (fig. 2A and B), with their limiting membranes still tightly enclosing the dense protein core. The second group of ACGs consisted of zymogen granules with an opened membrane (fig. 2C). Granule membranes which did not enclose a protein density formed a third group (fig. 2D). And finally, in the fourth group, also the membranes were absent, and only an isolated actin coat was apparent (fig. 2E). The latter three groups were distributed approximately evenly over the remaining 50% of ACGs. It should be noted that the first three morphological groups were also regularly observed without an actin coat.

The first two groups, that convincingly reveal zymogen granules with their dense inner cores, confirm that actin actually coats the granules, and that actin coat formation is intrinsic to the granules; an intact cellular environment is not a necessity. In particular, the group of intact zymogen granules shows that actin coating is a process that can take place early in the secretory response, and is likely to precede fusion with the plasma membrane. Further supporting this was the fact that ACGs also arose in the cytosolic fractions wherein plasma membrane is largely absent, and actin coating could not have occurred in response to membrane fusion.

Groups three and four, in which a protein core or even an enclosed vesicle is absent, are not obviously surrounding zymogen granules. However, since group two already contained an opened zymogen granule, it seems likely that the protein content can diffuse away, which would give rise to group three. Group three in its turn can give rise to group four by the flattening of the granule membrane over time, or the complete loss of it. However, the most persuading evidence that the groups are all linked came from cryo-electron tomographic reconstructions of correlated ACGs, which showed that the structure of the actin coats are identical in all three cases.

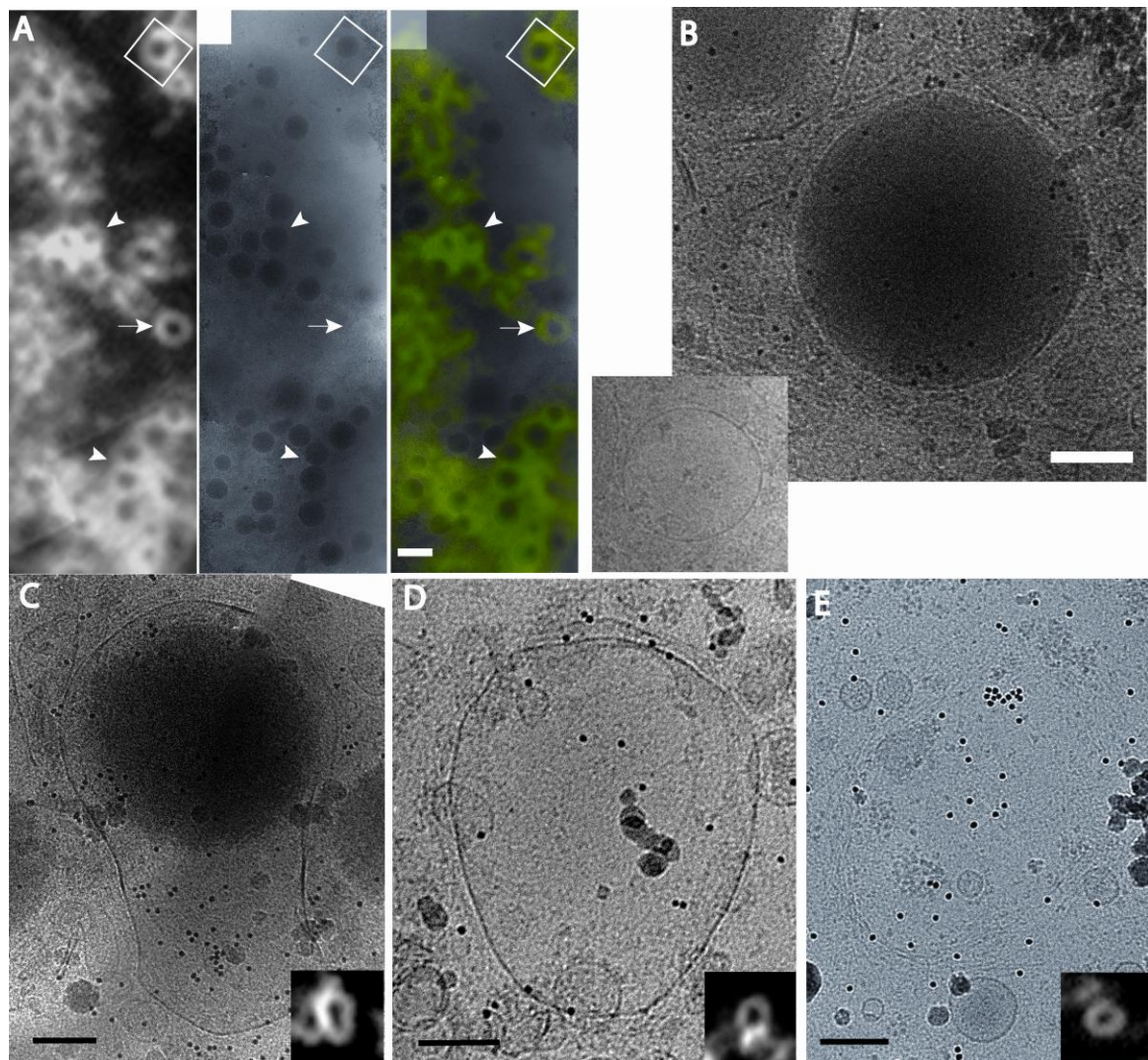


Figure 2. Cryo-CLEM of actin coats in pancreatic homogenates. A) Cryo-FM, cryo-EM and cryo-FM-EM overlay micrographs of stimulated pancreatic homogenate. Several actin rings (indicated by the arrow and the boxed area) and clustered actin rings (indicated by the arrowheads) can be observed. The actin coat in the boxed area surrounds a zymogen granule that is still intact, and is shown in (B). Because of the thickness of the specimen, the actin filaments can hardly be discerned in the projection image. The actin coat indicated by the arrow in (A), on the other hand, encloses a membrane structure that does not contain zymogen (inset in B). Figures C), D), and E) are cryo-electron micrographs, with associated cryo-FM micrographs in the insets, of actin coats around different morphological granules. The granule in C) displays the characteristic dense protein core of a zymogen granule, surrounded by a damaged membrane. Notice that the actin coat follows the outer membrane of the granule where it bulges outward. D) actin coated granule that clearly shows a damaged membrane, but lacks a protein core. E) actin coat where both granule core and membrane are seemingly missing. Scale bars represent 1 μm in A), 200 nm in B), and 200 nm in C), D) and E).

Actin forms a ring around opened granules

The thickness and electron denseness of the intact granules did not allow for cryo-electron tomography. However, the actin coats on the damaged granules all looked very similar, and might give a good indication of the structure of actin coats. The further ultrastructural characterization of the actin coats was therefore done on these actin assemblies (groups two through four).

Surprisingly, all cryo-electron tomograms revealed actin coats as being a ring of actin filaments surrounding the middle of the granule (fig. 3). The actin facing the inside of the ring formed a structured band of parallel actin filaments, whereas the actin facing the outside appeared less well organized, with rays of actin also directed outwards from the ring. The rings were 3 to 8 actin filaments thick and wide. Individual filaments were mostly between 0.5 and 2 μm long, and they partly overlap one another to form the complete ring. The distance between two parallel filaments was often small, around 15 nm measured from the center of one filament to the next. The filaments never displayed convincing branching points, and connections to the granule membrane were only rarely observed.

Since we concluded that the opened membranes of these three groups of actin coats are artifacts of the tissue preparation, we cannot assume with certainty that the actin surrounding intact zymogen granules is also shaped in a ring. This remains to be determined in future experiments. Nevertheless, the actin coats that we observed in cryo-electron tomograms do have a very reproducible morphology in all three groups that allowed tomography. The finding of an actin ring in these 3D observations is an interesting phenomenon that is worth considering in future experiment on the role of actin in regulated exocytosis.

Actin rings are surrounded by clathrin-coated vesicles

A surprising feature in the cryo-electron tomograms, were numerous clathrin-coated vesicles (CCVs) that surrounded the actin rings (fig. 3). The CCVs were always connected to an actin filament, which explains why they did not diffuse away in the homogenate. They were heterogeneous in structure; some being smaller, larger, spherical or longitudinal. There were between 5 and 20 CCVs in every tomogram, and all were located outside of the actin ring, never within it. The presence of CCVs specifically at sites of zymogen granule collapse shows that the *in vitro* environment allows clathrin, and likely other endocytosis-associated proteins, to be recruited to those specific locations.

Discussion

Actin coating *in vitro*

Several findings suggest that the actin coats we observe in homogenized pancreas correspond to the ACGs observed in earlier studies. The actin coats in fluorescence microscopy have the same appearance and diameter as those observed in pancreatic tissue sections and pancreatic acini (Tandon and De Lisle, 2004; Turvey and Thorn, 2004; Valentijn et al., 2000). In addition, they arose only after the addition of Ca^{2+} , ATP and GTP[γS], which mimic secretory stimulation, and activate GTP-binding proteins. The mentioned studies also show indirect evidence, by different

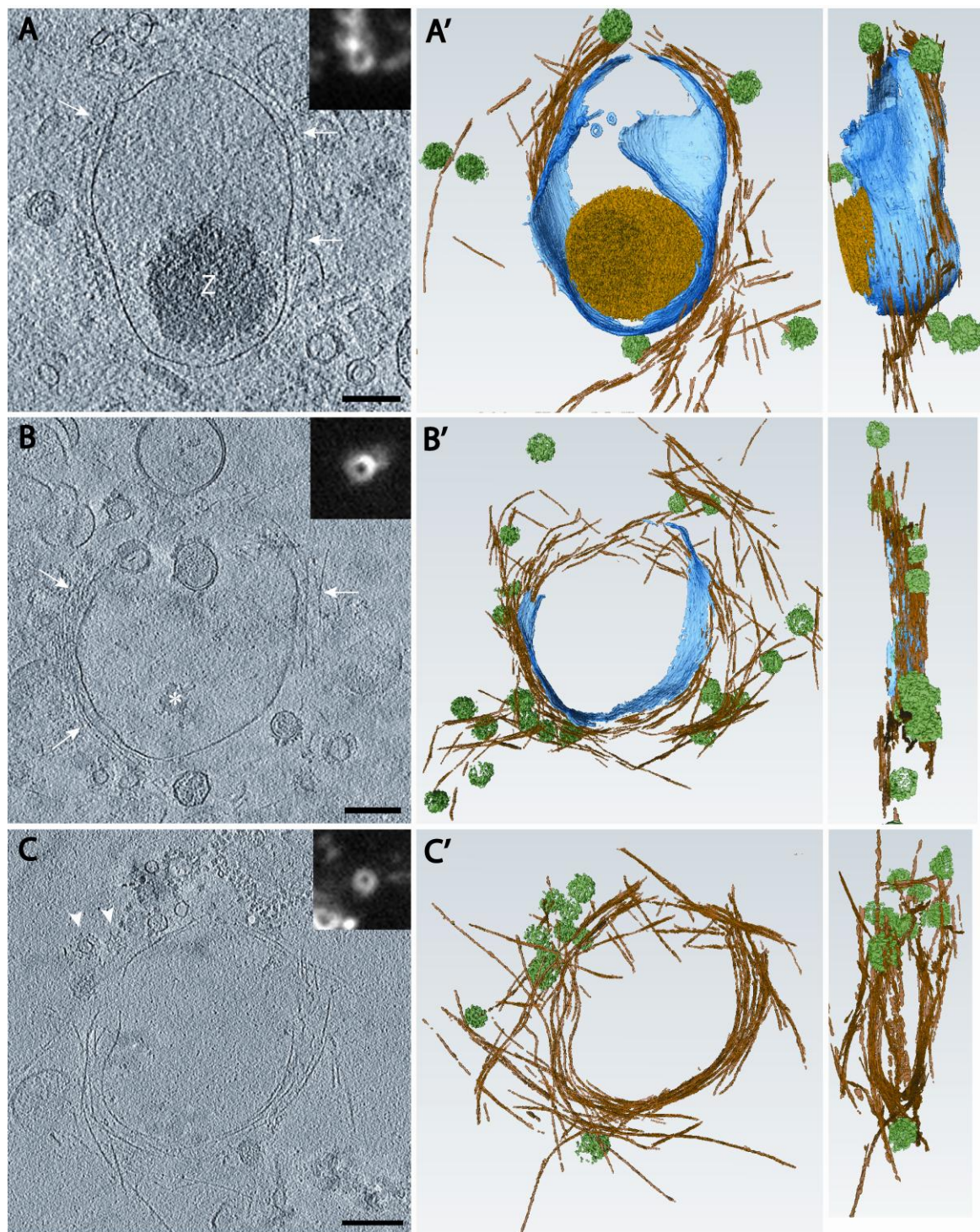


Figure 3. Correlated cryo-electron tomograms of actin coats with corresponding 3D models. The tomographic slices in (A), (B) and (C) are around 10 nm thick. Their cryo-FM counterparts are shown in the insets (5 x 5 μm). The three consecutive tomograms represent the three groups of actin coats that were observed; actin coats surrounding a granule with a dense zymogen core (A), actin coats surrounding a granule membrane (B) and actin coats where the surrounded granule is apparently missing. Front views ((A'), (B') and (C')), and side views ((A''), (B'') and (C'')) of the models show that the actin coats (brown) in all three cases consist of rings of long actin filaments several layers of actin thick. They also show that the tomograms contained multiple CCVs (green). The granule membranes in the tomograms are colored blue. Scale bars represent 200 nm.

fluorescent labeling methods, that actin coats surround zymogen granules, a finding that we can now confirm with direct evidence from electron microscopy. We therefore conclude that actin coated zymogen granules can develop in an *in vitro* environment, and that actin coat formation is therefore intrinsic to zymogen granules.

How did the actin coat assembly take place? We observed that ACGs surrounding intact zymogen granules still formed in the cytosol fractions, where all material left behind in the PNS was ultracentrifuged and discarded. This suggests that F-actin formation at the granule membrane proceeded by the polymerization of G-actin rather than the redistribution of F-actin. In accordance with this, actin coat formation around zymogen granules was blocked by inhibitors of actin polymerization (Nemoto et al., 2004). In addition, it has been described that zymogen granules in rest are surrounded by G-actin that is bound to the limiting granule membrane (Bendayan, 1985; Bendayan et al., 1982). Such a G-actin coat has also been described in oocyte secretory vesicles (Sokac et al., 2003), and was shown to still be bound to the membranes of chromaffin granules even after granule membrane isolation (Wilkins and Lin, 1981). The G-actin bound to the periphery of chromaffin granules acted as nucleation points for actin monomers to polymerize into F-actin (Wilkins and Lin, 1981), a role that is fulfilled in neuroendocrine cells by the actin nucleation complex Arp2/3 present on secretory granules (Gasman et al., 2004).

The above data indicate that actin coat assembly takes place after secretory stimulation, but before exocytosis. This idea is further supported by the finding that actin coats often enclose intact, mature zymogen granules, as seen by cryo-CLEM (fig. 2). This result is in contrast with other studies that have proposed that actin coating is a process that happens well after exocytosis (Nemoto et al., 2004; Sokac and Bement, 2006; Turvey and Thorn, 2004). The electron denseness of the protein cores in these granules illustrates that the protein did not mix with the buffer surrounding the granule. Therefore, the intact membrane is not a consequence of it resealing after having been opened in a possible event of dynamic fusion pore opening (Larina et al., 2007). Also, the presence of a small fusion pore in these granules that we simply cannot observe in a 2D projection image seems unlikely. First of all, in the case of a small fusion pore, the homogenization buffer would be allowed to enter (Larina et al., 2007), and the granules would have a dilated morphology. And, more convincingly, the cytosol fractions, which are largely free from plasma membrane with which granules could fuse, also contained intact ACGs. We therefore conclude that secretory stimulation is a sufficient trigger for actin coating of zymogen granules *in vitro*, and it may occur before exocytosis.

Cryo-EM of the zymogen granule pellets revealed that the granules had the tendency to cluster together. This tendency was also recognized earlier in the experiments, when centrifuged granule pellets were difficult to resuspend. The reason for this is unclear, but the clusters may have provided protection to the enclosed zymogen granules. The zymogen granules as well as ACGs that were seen to lie rather isolated always had damaged membranes. In accordance with this, zymogen granules have been described to be very sensitive to the shearing forces they are

inevitably exposed to during pellet resuspension (De Lisle et al., 1984; Scheele et al., 1987). A supplementary influencing effect of the tissue preparation, is that all the pellet resuspension steps were performed on unfixed material, which likely made the granules more vulnerable to the shearing forces.

The isolated, damaged granules, however sometimes did display clear actin coats around them, which offered the opportunity of cryo-electron tomography of these actin coats. Although these coats cannot be considered completely physiological, they are at least related to the intact ACGs, which were inaccessible for tomography. In all correlated cryo-electron micrographs and tomograms, the fluorescent actin coats appeared to be rings of long, overlapping, parallel actin filaments. This finding was unexpected, as data from fluorescence microscopy always suggested a sphere of actin enclosing the secretory granules. In accordance, the hypothetical models were mostly drawn as numerous short actin filaments forming a meshwork around a fusing granule (Sokac and Bement, 2006; Valentijn et al., 1999a). However, the actin ring did not show any signs of being a collapsed sphere: actin filaments, in whatever direction, were never observed within the ring. One might also argue that the surface tension of the thin layer of water forced a spherical actin meshwork into a ring. However, this surface tension is only present on the top of the sample; the bottom of the sample is protected by a formvar and carbon layer. An artifact like this would therefore have resulted in a half actin sphere, missing filaments only at the top of the sample. Furthermore, the orientation of the rings always being perpendicular to the viewing axis may well be explained by the surface tension at the air-water interface in the thin layer of ice. This likely causes the actin ring to have a preferred orientation, similar to large macromolecular complexes (Van Heel, 1987).

Nevertheless, we cannot completely rule out the possibility that the rings surrounding the damaged granules are somehow an artifact. Future experiments on the actin coats surrounding intact zymogen granules are therefore necessary to complement the above data. First of all, a mechanism can be searched that allows separation of the intact zymogen granules. For example, ultracentrifugation of the crude zymogen granule pellet in a Percoll gradient produces a more purified granule pellet (De Lisle et al., 1984; Rindler, 2006), where individual granules are likely separated in the Percoll. However, the electron density of the granules will still render cryo-electron tomography challenging in such samples. Additional requirements would therefore be the use of holey carbon support films instead of formvar films, and using a microscope with a higher acceleration voltage. Alternatively, tomography can be avoided by labeling actin with gold markers that can be observed in a 2D view. Although this doesn't allow ultrastructural examination, it would answer the question whether the actin coats around intact granules are also shaped in a ring. For ultrastructural examination of the coat, a step of vitreous sectioning may be included in the cryo-CLEM workflow to create thinner samples.

Biological explanations for an actin ring in exocytosis

Although additional evidence for an actin ring is yet to be acquired, the reproducible ultrastructure of the ring in 15 tomograms and even so many 2D images from four different experiments, and from granules in different stages of opening and collapse, led us to investigate, by means of a literature study, the possibility that an actin ring in regulated exocytosis is a physiological phenomenon.

The phenomenon of an actin ring in itself is not new. Well-known actin rings are the contractile rings associated with cytokinesis (Glotzer, 2005) and wound closure (Bement et al., 1993; Darenfed and Mandato, 2005). These rings, as the rings in our tomograms, are composed of parallel bundles of unbranched actin (Glotzer, 2005; Kamasaki et al., 2007), and the actin filaments in cytokinesis moreover have identical length distributions – mostly between 500 nm and 2 μm (Kamasaki et al., 2007). The similar ultrastructures would also suggest related functionalities. The actin rings in cytokinesis and wound healing have in common that the actin ring stabilizes an energetically unfavorable membrane structure; in cytokinesis it prevents the membrane from expanding outward, whereas in wound healing it prevents the widening of a wound in the cell. A consistent function that can be proposed for an actin ring in exocytosis is the stabilization of a fusion pore, to prevent a granule from a full collapse into the plasma membrane.

Interestingly, an actin ring is also constructed during the regulated exocytosis of oocyte secretory vesicles (Becker and Hart, 1999). Following exocytosis, the actin ring rapidly assembles around the exocytosing granule. The actin profiles encircled the full diameter of the oocyte granule, which are large in size, generally between 15 to 25 μm . Subsequently, the narrow, intense band of actin becomes decorated on the inside by a broadening actin meshwork, which slowly closes up the exocytic profile and restores the membrane. The complete process of membrane closure by the actin band takes around 30-60 seconds, in contrast to fusion pore opening and exocytosis, which covers only a few seconds. The actin ring was assigned a function in the stabilization of the exocytic profile, while regulating the remodeling of the plasma membrane, and perhaps the compensatory endocytosis of granule membrane. The illustration of this actin ring is remarkably similar to the actin rings observed in this study for zymogen granules. Like the oocyte rings, they are compact, thin actin assemblies that delineate the full diameter of the enclosed granule. Also in accordance, the fusion dynamics of oocytes and zymogen granules are very similar. Imaging of single exocytotic events reveals that the time required for exocytosis is less than 1 second (Ishihara et al., 2000; Thorn and Parker, 2005), whereas, following exocytosis, empty exocytic profiles persist for several minutes before slowly decreasing in size (Nemoto et al., 2001; Thorn and Parker, 2005; Thorn et al., 2004).

One important question still remains; if an actin ring is indeed involved in regulated exocytosis, how does it fit with published data that show spheres of actin enclosing the secretory granules? The actin spheres were suggested to stabilize the exocytosing granule membrane (Nemoto et al.,

2004; Tandon and De Lisle, 2004). A possible answer is again illustrated by the oocyte exocytosis described by Becker and Hart (1999). The actin band in this study is formed by two pools of actin: a narrow, intense ring of actin at the initial fusion pore, and a broad, continuous band of actin that widens to the center of the ring to close the pore. Such a two-steps process has also been shown in the exocytosis of post-lysosomes in *Dictyostelium* cells (Lee and Knecht, 2002). In this case, a faint coat of filamentous actin prior to exocytosis changes into a brightly fluorescent actin coat after the onset of exocytosis. In the case of zymogen granules, a primary actin ring may similarly be supplemented with a second pool of actin that forms a spherical meshwork around the exocytic profile.

Clathrin Coated Vesicles

An intriguing finding in the cryo-electron tomograms was the presence of multiple CCVs along the outside of the actin ring. The CCVs were always attached to a actin filament, which explains why they remained associated with the actin assemblies. It shows that clathrin present in the homogenates was somehow recruited to sites of damaged zymogen granules, where they initiated clathrin-mediated endocytosis. Although CCVs are known to take care of plasma membrane retrieval following the regulated exocytosis of zymogen granules (Herzog and Farquhar, 1977; Herzog and Reggio, 1980; Valentijn et al., 1999b), the zymogen granules observed *in vitro* did not undergo regulated exocytosis, and the granule membrane did not incorporate into the plasma membrane. Nevertheless, a recent study on compensatory membrane retrieval in chromaffin cells raised a related explanation (Ceridono et al., 2011). The study shows that, following full collapse exocytosis of the dense-core granules, the granule membrane composites do not mix with the plasma membrane, but remain patched together. These patches of granule membrane are subsequently specifically recognized and taken up by clathrin-mediated endocytosis. The findings illustrate that clathrin can somehow be recruited to specific membrane compositions. It is therefore possible that the membrane of the damaged zymogen granules elicited the same response. Interestingly, the study also concluded that actin participates in the internalization of the CCVs.

In conclusion, this communication shows for the first time that cryo-CLEM enables the identification of rare events that are difficult to localize in EM, and gave insight in the high resolution details of exocytosis-associated actin coats around zymogen granules. The actin coating occurred in response to secretory stimulation, and membrane fusion with plasma membrane was not necessary for its onset. Although the ultrastructure of the actin coats could not be studied on intact zymogen granules, the actin coats on opened zymogen granules reproducibly show a compact actin ring that surrounds the full diameter of the granules. The ring is composed of long bundles of actin filaments, very comparable to actin rings described in literature to associate cytokinesis, wound healing and exocytosis of oocyte granules. The present study is not yet completed to the point where a decisive answer can be provided on the physiological relevance of the actin rings. However, it does present interesting novel findings that may already

inspire other exocytosis-related studies to reconsider their current hypotheses concerning the role of actin.

References

- Aunis, D., and M.F. Bader, 1988. The cytoskeleton as a barrier to exocytosis in secretory cells. *J Exp Biol* 139: 253-66.
- Becker, K.A., and N.H. Hart, 1999. Reorganization of filamentous actin and myosin-II in zebrafish eggs correlates temporally and spatially with cortical granule exocytosis. *J Cell Sci* 112 (Pt 1): 97-110.
- Bement, W.M., P. Forscher, and M.S. Mooseker, 1993. A novel cytoskeletal structure involved in purse string wound closure and cell polarity maintenance. *J Cell Biol* 121: 565-78.
- Bendayan, M., 1985. Ultrastructural localization of cytoskeletal proteins in pancreatic secretory cells. *Can J Biochem Cell Biol* 63: 680-90.
- Bendayan, M., N. Marceau, A.R. Beaudoin, and J.M. Trifaro, 1982. Immunocytochemical localization of actin in the pancreatic exocrine cell. *J Histochem Cytochem* 30: 1075-8.
- Bi, G.Q., R.L. Morris, G. Liao, J.M. Alderton, J.M. Scholey, and R.A. Steinhardt, 1997. Kinesin- and myosin-driven steps of vesicle recruitment for Ca²⁺-regulated exocytosis. *J Cell Biol* 138: 999-1008.
- Burgoyne, R.D., and T.R. Cheek, 1987. Reorganisation of peripheral actin filaments as a prelude to exocytosis. *Biosci Rep* 7: 281-8.
- Cai, H., K. Reinisch, and S. Ferro-Novick, 2007. Coats, tethers, Rabs, and SNAREs work together to mediate the intracellular destination of a transport vesicle. *Dev Cell* 12: 671-82.
- Ceridono, M., S. Ory, F. Momboisse, S. Chasserot-Golaz, S. Houy, V. Calco, A.M. Haeberle, V. Demais, Y. Bailly, M.F. Bader, and S. Gasman, 2011. Selective recapture of secretory granule components after full collapse exocytosis in neuroendocrine chromaffin cells. *Traffic* 12: 72-88.
- Darenfed, H., and C.A. Mandato, 2005. Wound-induced contractile ring: a model for cytokinesis. *Biochem Cell Biol* 83: 711-20.
- De Lisle, R.C., I. Schulz, T. Tyrakowski, W. Haase, and U. Hopfer, 1984. Isolation of stable pancreatic zymogen granules. *Am J Physiol* 246: G411-8.
- Ferro-Novick, S., and R. Jahn, 1994. Vesicle fusion from yeast to man. *Nature* 370: 191-3.
- Gasman, S., S. Chasserot-Golaz, M. Malacombe, M. Way, and M.F. Bader, 2004. Regulated exocytosis in neuroendocrine cells: a role for subplasmalemmal Cdc42/N-WASP-induced actin filaments. *Mol Biol Cell* 15: 520-31.
- Glotzer, M., 2005. The molecular requirements for cytokinesis. *Science* 307: 1735-9.
- Herzog, V., and M.G. Farquhar, 1977. Luminal membrane retrieved after exocytosis reaches most golgi cisternae in secretory cells. *Proc Natl Acad Sci U S A* 74: 5073-7.
- Herzog, V., and H. Reggio, 1980. Pathways of endocytosis from luminal plasma membrane in rat exocrine pancreas. *Eur J Cell Biol* 21: 141-50.
- Ishihara, Y., T. Sakurai, T. Kimura, and S. Terakawa, 2000. Exocytosis and movement of zymogen granules observed by VEC-DIC microscopy in the pancreatic tissue en bloc. *Am J Physiol Cell Physiol* 279: C1177-88.
- Jerdeva, G.V., K. Wu, F.A. Yarber, C.J. Rhodes, D. Kalman, J.E. Schechter, and S.F. Hamm-Alvarez, 2005. Actin and non-muscle myosin II facilitate apical exocytosis of tear proteins in rabbit lacrimal acinar epithelial cells. *J Cell Sci* 118: 4797-812.
- Kamasaki, T., M. Osumi, and I. Mabuchi, 2007. Three-dimensional arrangement of F-actin in the contractile ring of fission yeast. *J Cell Biol* 178: 765-71.

- Kremer, J.R., D.N. Mastrorarde, and J.R. McIntosh, 1996. Computer visualization of three-dimensional image data using IMOD. *J Struct Biol* 116: 71-6.
- Larina, O., P. Bhat, J.A. Pickett, B.S. Launikonis, A. Shah, W.A. Kruger, J.M. Edwardson, and P. Thorn, 2007. Dynamic regulation of the large exocytotic fusion pore in pancreatic acinar cells. *Mol Biol Cell* 18: 3502-11.
- Lee, E., and D.A. Knecht, 2002. Visualization of actin dynamics during macropinocytosis and exocytosis. *Traffic* 3: 186-92.
- Malsam, J., S. Kreye, and T.H. Sollner, 2008. Membrane fusion: SNAREs and regulation. *Cell Mol Life Sci* 65: 2814-32.
- Martens, S., M.M. Kozlov, and H.T. McMahon, 2007. How synaptotagmin promotes membrane fusion. *Science* 316: 1205-8.
- Maupin-Szamier, P., and T.D. Pollard, 1978. Actin filament destruction by osmium tetroxide. *J Cell Biol* 77: 837-52.
- Melia, T.J., Jr., 2007. Putting the clamps on membrane fusion: how complexin sets the stage for calcium-mediated exocytosis. *FEBS Lett* 581: 2131-9.
- Miklavc, P., O.H. Wittekindt, E. Felder, and P. Dieltl, 2009. Ca²⁺-dependent actin coating of lamellar bodies after exocytotic fusion: a prerequisite for content release or kiss-and-run. *Ann N Y Acad Sci* 1152: 43-52.
- Muallem, S., K. Kwiatkowska, X. Xu, and H.L. Yin, 1995. Actin filament disassembly is a sufficient final trigger for exocytosis in nonexcitable cells. *J Cell Biol* 128: 589-98.
- Nemoto, T., T. Kojima, A. Oshima, H. Bito, and H. Kasai, 2004. Stabilization of exocytosis by dynamic F-actin coating of zymogen granules in pancreatic acini. *J Biol Chem* 279: 37544-50.
- Nemoto, T., R. Kimura, K. Ito, A. Tachikawa, Y. Miyashita, M. Iino, and H. Kasai, 2001. Sequential-replenishment mechanism of exocytosis in pancreatic acini. *Nat Cell Biol* 3: 253-8.
- Pickett, J.A., and J.M. Edwardson, 2006. Compound exocytosis: mechanisms and functional significance. *Traffic* 7: 109-16.
- Poucell-Hatton, S., P.S. Perkins, T.J. Deerinck, M.H. Ellisman, W.G. Hardison, and S.J. Pandol, 1997. Myosin I is associated with zymogen granule membranes in the rat pancreatic acinar cell. *Gastroenterology* 113: 649-58.
- Rindler, M.J., 2006. Isolation of zymogen granules from rat pancreas. *Curr Protoc Cell Biol* Chapter 3: Unit 3 18.
- Rothman, J.E., and T.H. Sollner, 1997. Throttles and dampers: controlling the engine of membrane fusion. *Science* 276: 1212-3.
- Scheele, G., G. Adler, and H. Kern, 1987. Exocytosis occurs at the lateral plasma membrane of the pancreatic acinar cell during supramaximal secretagogue stimulation. *Gastroenterology* 92: 345-53.
- Segawa, A., and S. Yamashina, 1989. Roles of microfilaments in exocytosis: a new hypothesis. *Cell Struct Funct* 14: 531-44.
- Sokac, A.M., and W.M. Bement, 2006. Kiss-and-coat and compartment mixing: coupling exocytosis to signal generation and local actin assembly. *Mol Biol Cell* 17: 1495-502.
- Sokac, A.M., C. Co, J. Taunton, and W. Bement, 2003. Cdc42-dependent actin polymerization during compensatory endocytosis in *Xenopus* eggs. *Nat Cell Biol* 5: 727-32.
- Tandon, C., and R.C. De Lisle, 2004. Apactin is involved in remodeling of the actin cytoskeleton during regulated exocytosis. *Eur J Cell Biol* 83: 79-89.

- Taunton, J., 2001. Actin filament nucleation by endosomes, lysosomes and secretory vesicles. *Curr Opin Cell Biol* 13: 85-91.
- Thorn, P., and I. Parker, 2005. Two phases of zymogen granule lifetime in mouse pancreas: ghost granules linger after exocytosis of contents. *J Physiol* 563: 433-42.
- Thorn, P., K.E. Fogarty, and I. Parker, 2004. Zymogen granule exocytosis is characterized by long fusion pore openings and preservation of vesicle lipid identity. *Proc Natl Acad Sci U S A* 101: 6774-9.
- Turvey, M.R., and P. Thorn, 2004. Lysine-fixable dye tracing of exocytosis shows F-actin coating is a step that follows granule fusion in pancreatic acinar cells. *Pflugers Arch* 448: 552-5.
- Valentijn, J.A., K. Valentijn, L.M. Pastore, and J.D. Jamieson, 2000. Actin coating of secretory granules during regulated exocytosis correlates with the release of rab3D. *Proc Natl Acad Sci U S A* 97: 1091-5.
- Valentijn, K., J.A. Valentijn, and J.D. Jamieson, 1999a. Role of actin in regulated exocytosis and compensatory membrane retrieval: insights from an old acquaintance. *Biochem Biophys Res Commun* 266: 652-61.
- Valentijn, K.M., F.D. Gumkowski, and J.D. Jamieson, 1999b. The subapical actin cytoskeleton regulates secretion and membrane retrieval in pancreatic acinar cells. *J Cell Sci* 112 (Pt 1): 81-96.
- Van Heel, M., 1987. Angular reconstitution: a posteriori assignment of projection directions for 3D reconstruction. *Ultramicroscopy* 21: 111-23.
- van Weeren, L., A.M. de Graaff, J.D. Jamieson, J.J. Batenburg, and J.A. Valentijn, 2004. Rab3D and actin reveal distinct lamellar body subpopulations in alveolar epithelial type II cells. *Am J Respir Cell Mol Biol* 30: 288-95.
- Wilkins, J.A., and S. Lin, 1981. Association of actin with chromaffin granule membranes and the effect of cytochalasin B on the polarity of actin filament elongation. *Biochim Biophys Acta* 642: 55-66.
- Yu, H.Y., and W.M. Bement, 2007. Control of local actin assembly by membrane fusion-dependent compartment mixing. *Nat Cell Biol* 9: 149-59.